SPE 83960

Variations of Gas-Condensate Relative Permeability with Production Rate at Near Wellbore Conditions: A General Correlation

M. Jamiolahmady, A. Danesh, G. Henderson, and G.D. Tehrani

Abstract

It has been demonstrated, first by this laboratory and subsequently by other researchers, that the gas and condensate relative permeability can increase significantly by increasing rate contrary to the common understanding. There are now a number of correlations in the literature and commercial reservoir simulators accounting for the positive effect of coupling and the negative effect of inertia at near wellbore conditions. The available functional forms estimate the two effects separately and include a number of parameters, which should be determined using measurements at high velocity conditions. Measurements of gas-condensate relative permeability at simulated near wellbore conditions are very demanding and expensive.

Intruduction

The process of condensation around the wellbore in a gas-condensate reservoir, when the pressure falls below the dew point, creates a region in which both gas and condensate phases flow. The flow behaviour in this region is controlled by the viscous, capillary and inertial forces. This along with the presence of condensate in all the pores dictate a flow mechanism that is different to that of gas-oil and also gas-condensate in the bulk of the reservoir[1]. Accurate determination of gas-condensate relative permeability (k_r) values, which is very important in well deliverability estimates, is a major challenge and requires a different approach compared to that for conventional gas-oil systems.

It has been widely accepted that relative permeability (k_r) values at low values of interfacial tension (IFT) are strong functions of IFT as well as fluid saturation[2-5]. Danesh et al.[6] were first to report the improvement of relative permeability of condensing systems due to an increase in velocity as well as that caused by a reduction in interfacial tension. This flow behaviour, named as the positive coupling effect, was subsequently confirmed experimentally by other investigators[7-10]. Jamiolahmady et al.[11] were first to study the positive coupling effect mechanistically capturing the competition of viscous and capillary forces at the pore level where there is a simultaneous flow of the two phases with intermittent opening and closure of gas passage by condensate. Jamiolahmady et al.[12] developed a steady-dynamic network model capturing this flow behaviour and predicted some k_r values, which were quantitatively comparable with the experimentally measured values.

There are also several empirical correlations in the literature and commercial simulators accounting for the positive effect of coupling at near wellbore conditions as a function of capillary number (ratio of viscous to capillary forces). These correlations can be divided into two main classes: (1) using Corey functions in which the Corey coefficients are interpolated between the immiscible and miscible limits[9,13] and (2) interpolation between miscible and immiscible relative permeability curves[14-16]. In both methods the interpolation is weighted by capillary number (Nc) dependent functions. Blom and Haggort[17] reviewed fifteen different correlations, all of which had capillary number and saturation as the main independent variables.

At high velocities where the inertial effect (non-Darcy flow) is significant the competition of inertial and coupling effects complicates the flow in this region even further. Henderson et al.[18], through some steady state k_r measurements, confirmed the significant effect of positive coupling effect even at very high velocities contrary to the conventional view that k_r would reduce with increasing velocity. They observed that the presence of condensate initially decreased the permeability due to inertia, before the positive coupling effect became dominant.

Henderson et al.[19] calculated the contribution of inertia at high velocities by subtracting the pressure loss predicted by the coupling effect from the experimentally measured values in this Laboratory. This difference is equivalent to the value of additional term in Forchhemier equation, which includes the two-phase inertia factor (β_g). Then, they developed a correlation for calculating the two-phase inertial factor for

gas-phase only, as the inertial effect is widely accepted to be insignificant for condensate phase.

Whitson et al. [20] also presented a k_{rg} correlation as a function of ratio of gas to condensate relative permeabilities (k_{rg}/k_{rL}) and Nc including the effect of inertia at high velocities. In the expressions for quantifying the positive coupling effect there are several empirical constants, which have been determined by tuning their model to a limited number of published data. The effect of additional pressure loss at higher velocities is attributed to inertia. The inertial effect is reflected in the effective relative permeability and includes β_g, which requires a separate formulation for its calculation. This formulation was borrowed from literature. Furthermore, their model is more suitable for rich gas-condensate systems where the flow of condensate is significant (krL>>0).

App and Mohanty[21] generated some synthetic ''experimental'' data through some numerical simulations over a wide range of capillary number variation. In creating the production data during this exercise (referred to as forward modelling) they selected a Corey type k_r functional form with capillary number dependent coefficients and a β_g-k_{rg} relationship for inertial resistance. In this part, the source of the required input parameters for these functional forms were not discussed. They then introduced some simplified correlations to represent both the gas and condensate relative permeabilities. Effective relative permeabilities, which included the inertial effect, were then history-matched to the synthetic data through non-linear regression. In their approach the correlations were partitioned into high-capillary-number (the miscible limit) region and the low capillary-number (immiscible) dependent region. Therefore, they have four different formulations for the relative permeabilities of gas and condensate phases. In these expressions, the main variables are saturation, Reynolds number (ratio of inertial to viscous forces) and the capillary number. There are also four case dependent constants and the calculation of Reynolds number requires an extra expression to estimate β_g, which was barrowed from literature.

The main difficulty in properly accounting for the inertial effect in all the reported correlations is the requirement for an accurate estimate of β_g. There are numerous correlations in the literature for calculating β_g [12,22]. These correlations relate the variation of β_g mainly to that of S_g and/or k_{rg}. However, most of the correlations used in the studies conducted for gas-condensate systems are open to question for a number of reasons. Some of the original formulations have been developed mainly for gas-water systems, with the water being the immobile phase. The β_g formulation, which is presented by Ali. et al.[9], is based on the measurements conducted using condensing systems but the condensate was assumed to be immobile. To the best of our knowledge the β_g formulation developed by Al-Kharousi[23] is the first to use the steady state gas condensate experimental measurements at high velocities. He also evaluated the accuracy of prediction of β_g by many different correlations and concluded that their application was

limited to the data they had been developed for and their application to other systems could lead to highly erroneous results.

In summary all the available correlations for estimating the relative permeability of gas condensate systems lack generality, i.e. there are core specific coefficients, and require some expensive relative permeability measurements. Furthermore, there are major difficulties in properly acknowledging the coupling and inertial effects simultaneously, which are in competition over a wide range of velocity variation with a gradual shift between the dominant effect of one to the other. Therefore, the aim of this work is twofold:

(1) To develop a correlation, which expresses the combined effect of the positive coupling and negative inertia based on a sound physical ground.
(2) To provide reliable information on variations of relative permeability at near wellbore conditions with no requirements for complex and expensive measurements. That is, the parameters of the proposed correlation are either universal, applicable to all types of rocks, or can be determined from commonly measured petrophysical data.

Recent experimental findings in this laboratory[24] indicate that measured gas-condensate relative permeability values on cores of different characteristics become more similar if expressed in terms of fractional flow instead of the common method of using saturation as independent variable. This would make a limited number of rock curves adequate for reservoir studies. Furthermore, the fractional flow is determined by fluid composition and prevailing pressure, which are more readily available information for a reservoir, whereas the fluid saturation depends on the rock properties. Hence, we have used a large data bank of gas-condensate relative permeability measurements to develop a general correlation accounting for the combined effects of coupling and inertia as a function of fractional flow. In this new approach, the gas relative permeability is interpolated between a base and a miscible fluid curve. The base curve is measured at a high value of interfacial tension and low velocity (commonly measured data), which then is corrected for the effect of inertia using a correlation, that is developed in this work. The miscible curve is a calculated curve accounting for the inertial effect. The interpolation function expresses the dependency of the relative permeability to velocity and interfacial tension. The condensate relative permeability is linked to that of gas by the fractional flow relation, thereby eliminating the need for two separate correlations.

Structure of Correlation

In a two-phase flow system one can apply the same flow equation as that for a single-phase flow, by replacing the absolute permeability (k) with the effective permeability (k_e) and replacing the inertial factor of a core for single-phase flow (β) with that of two-phase (β_j) flow for each of the flowing phases as follows:

$$\left[\nabla P = \frac{\mu}{k_e}V + \beta\rho|V|V\right]_j \qquad j = L, g \qquad (1)$$

with subscript L for condensate and g for gas.
Rearranging this equation we obtain:

$$\left\{V = \frac{k\nabla P}{\mu}\left(\frac{k_e/k}{1+\frac{\beta\rho k_e}{\mu}|V|}\right) = \frac{k\nabla P}{\mu}A\right\}_j . \qquad (2)$$

Comparing Darcy's law for two-phase flow, with Equation 2 suggests that A_j is equivalent to k_r of each phase. Generally, we intend to make no distinction between the relative permeability reported at low velocity values and those measured at high velocities wherein the inertial and coupling effects are significant. Therefore, hereafter the term k_r replaces A in our equation unless otherwise stated.

In the present fractional flow based correlation, gas relative permeability is interpolated between the base curve and the miscible-fluids curve using an interpolation function Y_g, as follows:

$$k_{rg} = Y_g k_{rgb} + (1-Y_g)k_{rgm} . \qquad (3)$$

This simple interpolation approach has been favoured by many investigators for expressing the coupling effect on k_r of gas-condensate systems at different values of capillary number, for it allows a direct insight into the variation of relative permeability and is most suited for calibrating a large number of data points. The main disadvantage of this type of correlation is attributed to its difficulty in ensuring a zero k_{rg} value at saturation values below S_{gr} at all conditions, which was overcome by adjustment of miscible curve using variable residual gas saturation. This draw back is eliminated here as the correlation is based on total fractional flow, which ensures zero k_r values for the end points where the flow of one of the phases ceases.

The fractional flow used in this study is the ratio of gas rate to total flow rate (GTR) expressed as,

$$GTR = \frac{Q_g}{Q_g + Q_L} = \frac{V_g}{V_L + V_g} . \qquad (4)$$

Substituting from Equation 2 into 4, results in a GTR expression, which is a function of k_r and μ of the two flowing phases as follows:

$$GTR = \frac{\left[\dfrac{k_r}{\mu}\right]_g}{\left[\dfrac{k_r}{\mu}\right]_L + \left[\dfrac{k_r}{\mu}\right]_g} . \qquad (5)$$

Solving the above equation for k_{rL} gives:

$$k_{rL} = \left[\frac{\mu_L k_{rg}}{\mu_g}\right]\left[\frac{1-GTR}{GTR}\right] . \qquad (6)$$

Therefore, when k_{rg} is separately determined as a function of GTR, the use of this equation gives the corresponding k_{rL} at the same value of GTR, thereby eliminating the need for a separate correlation for condensate phase. This is one of the advantages of the proposed approach.

Miscible Gas Relative Permeability Curve (k_{rgm}).
At miscible conditions the fluid properties of the two phases are similar, i.e.

$$\rho_m = \rho_{sm} = \rho_{gm} \qquad \& \qquad \mu_m = \mu_{sm} = \mu_{gm} \qquad (7)$$

where 'm' refers to miscible and 'sm' refers to a case where the total miscible gas and liquid phases are considered as a single phase flowing through a core with,

$$k = k_{esm} \qquad \& \qquad \beta = \beta_{sm} . \qquad (8)$$

From Equation 4, V_{gm} and V_{sm} are related by,

$$V_{gm} = V_{sm}GTR . \qquad (9)$$

Equating the right hand side of Equation 1 for both miscible gas phase and single phase, i.e. $\nabla P_{sm} = \nabla P_{gm}$, ignoring the inertial term (second term), for the time being, and substituting from Equations 7 to 9 we obtain:

$$k_{egm} = kGTR . \qquad (10)$$

Equating the right hand side of Equation 1 for both miscible gas phase and single phase, i.e. $\nabla P_{sm} = \nabla P_{gm}$, this time including the inertial term (second term), and substituting from Equations 7 to 10 gives:

$$\beta_{gm} = \frac{\beta}{[GTR]^2} . \qquad (11)$$

Combining Equations 10 to 11 with Equation 2, written for the miscible gas phase we obtain:

$$k_{rgm} = \left(\frac{GTR}{1+\beta\rho_m\left(\dfrac{k}{\mu_m}\right)|V|_{sm}}\right) . \qquad (12)$$

In Equation 12 the required miscible fluid properties (i.e. density, ρ_m, and viscosity, μ_m) are not easily available. However, we know that as pressure falls below the dew point

the density and viscosity of the gas phase will be smaller than their values at the dew point pressure, which themselves will be different form those at the critical point, where the fluids are miscible. In a sensitivity study it was noticed that the arithmetic average of the fluid properties of gas and condensate at any given pressure is a good approximation of the average value at the dew point over a significant pressure range below the dew point. That is, the average values are almost equal at all the pressure ranges with deviation being much smaller as pressure approaches the dew point pressure. These estimated dew point average properties are themselves close to the values at the miscible (critical) conditions for binary systems where the critical point can be reached by changing the composition (saturation pressure).

Base Relative Permeability Curve for Gas (k_{rgb}).
The base relative permeability curve is the measured curve at the lowest practicable velocity level and the highest realistic IFT value, $(k_{rgb})_{meas}$, which is then modified for the effect of inertia, $(k_{rgb})_{iner}$ when the velocity is high. The main difficulty in including the inertial effect is the lack of information on the gas two-phase Forchheimer factor, β_g, Equation 1. Different options were considered and finally an approach similar to that used for the miscible curve was adopted. That is, the inertial pressure drop was calculated by using the single-phase β value, the total velocity, V_T, and the summation of total momentum inflow as follows:

$$\nabla P_{iner} = \beta \left[\left(\rho |V| \right)_g + \left(\rho |V| \right)_L \right] V_T . \qquad (13)$$

Substituting for gas and liquid velocities using the definition of GTR, Equation 2, and replacing both ρ_g and ρ_L by ρ_{ave} we obtain:

$$\nabla P_{iner} = \beta \left[\rho_g GTR + \rho_L (1 - GTR) \right] V|_T V_T \\ = \beta \rho_{ave} |V|_T V_T \qquad (14)$$

Hence, after some mathematical manipulation on Equation 14, similar to that done to obtain Equation 12, k_{rgb} modified for the effect of inertia is calculated by,

$$\left(k_{rgb} \right)_{iner} = \left(\frac{\left(k_{rgb} \right)_{meas}}{1 + \dfrac{\beta \rho_{ave} k \left(k_{rgb} \right)_{meas}}{GTR \mu_g} |V|_T} \right) . \qquad (15)$$

where $(k_{rgb})_{meas}$ is the base relative permeability measured at low velocity (with no inertia effect). This modification correctly extends the correlation to the single-phase flow limit at the base IFT value at any given velocity.

It should be noted that although the above analysis is for $S_{wi}=0$ but the same formulations are valid for $S_{wi}>0$, with $k_{eg}(S_{wi})$ and $\beta_g(S_{wi})$ replacing k and β, respectively. Furthermore, due to the presence of the rock properties (k & β) in Equations 12 & 15, there are a base and a miscible

relative permeability versus GTR curve for each core at any velocity value.

Y_g Formulation.
To determine the functional form of Y_g for use in Equation 3, we used the experimentally measured k_{rg} values for Clashach and Berea sandstone cores. A considerable amount of information is available at different conditions for these two cores in this laboratory. Tables 1 and 2 summarise the basic test data for the twenty sets of measurements conducted on these two cores.

There was only one measured inertial factor $\beta(S_{wi})$ which was obtained for the Clashach wet core sample with $S_{wi}=33\%$ (Test 6 in Table 1). To estimate the $\beta(S_{wi})$ values for the other wet core tests (i.e. with S_{wi} in the core sample), as shown in Tables 1 and 2, different options were examined. Finally, we adopted a modified form of the formulation recommended by Coles and Hartman[25] who recently have done some measurements for β of a series of core samples. They suggested the extension of the general form in the literature for β to $\beta(S_{wi})$ as follows:

$$\beta_{eff} = Ck_{eff}^{B} \phi_{eff}^{A} . \qquad (16)$$

In their study the values for A, B and C were determined as 0.448, –1.88 and 1.07E12, respectively, where k is in mD, ϕ in fraction and β in ft^{-1}.

We applied Equation 16 for both dry and wet samples eliminating the constant C as follows,

$$\beta(S_{wi}) = \beta \left[\frac{k}{k(S_{wi})} \right]^{1.88} \left[1 - S_{wi} \right]^{0.448} . \qquad (17)$$

Applying Equation 17 to Experiment number 6 under-predicts $\beta(S_{wi})$ by 13%, which seems a reasonable error for beta determination and was the least deviation among different options considered in this exercise. Therefore, the estimated $\beta(S_{wi})$ values reported here were obtained using Equation 17.

The available weight functions in the interpolation approach, used to predict k_r of condensing systems, is dependent on capillary number ratio, the ratio of the prevailing capillary number to its base value ($N_{cr}=N_c/N_{c_{base}}$), with different core specific constants for gas and condensate phases. There are several definitions in the literature[17] for the capillary number. Based on a comprehensive sensitivity study different definitions of capillary number were examined and it was concluded that the following Nc definition:

$$Nc = \frac{k\Delta P}{\phi \sigma L} = \frac{k|\nabla P|}{\phi \sigma} \qquad (18)$$

was more suitable to represent the ratio of viscous and capillary forces and proved to correlate the data more consistently.

Figure 1 shows the calculated Y_g versus capillary number ratio, Ncr for dry Clashach core tests, Experiments 1 to 5. These Y_g values have been calculated for any experimentally measured k_{rg} value by rearranging Equation 1 as follows:

$$Y_g = \frac{(k_{rg})_{meas} - k_{rgm}}{(k_{rgb})_{iner} - k_{rgm}} . \tag{19}$$

where $(k_{rg})_{meas}$ is the measured k_{rg} at a given (non-base) IFT and velocity and k_{rgm} and $(k_{rgb})_{iner}$ were calculated at any velocity level and GTR value by Equations 12 and 15, respectively.

The data in this figure demonstrates that the bulk of data follows a consistent trend but very scattered. In this figure there are also two trends, which are different from the main trend followed by the majority of data points. In the first category (marked '1' on Figure 1) at low IFT values the data points at high GTR values have a very low Y_g value. That is, $k_{rg} \gg k_{rgb}$ at same GTR and velocity but lower IFT values, as shown in Figure 2, which a plot of k_{rg} measured at three different IFT values for the same base velocity. After a careful examination of these data points it was concluded that this trend could be attributed to a different flow mechanism occurred by the presence of condensate in the micro-pores of the core. In the case of Clashach core, where there is a very small percentage of these pores, the contribution is limited to GTR=0.995, Table 3, but, for the Berea core with a higher share of these small tight pores, the data at lower GTR values have also been affected, Table 4. In the presence of connate water these small pores are filled with water and the contribution of very small pores filled with condensate is insignificant even at high GTR values. Note that fewer data points are affected for the Berea core sample with S_{wi}=26% compared to the corresponding test for the dry core sample at these conditions, Table 4. Furthermore, as IFT increases whereby the flow is mostly dominated by the bigger pores less contribution is noted by the condensate present in these small pores. These data points were not included in the development of the first part of the correlation at this stage but they are employed later to modify the correlation.

The second type of deviation contains data points at very high GTR having Y_g greater than unity indicating the dominant effect of inertia (i.e. k_{rg} is less than $(k_{rgb})_{iner}$), which is more pronounced for cores with higher β values. This is mainly due to the use of single-phase inertial factor (β) in adjusting k_{rgb} for inertia. This deviation is less pronounced compared to the first one and is limited to a very low range of GTR values for dry core samples at base IFT (IFT=0.852 mNm^{-1}) where inertia has the dominant effect.

Careful examination of Y_g values following the main trend, labeled hereafter as $(Y_g)_{Main}$, suggested that $(Y_g)_{Main}$ is not only a function of Ncr but also IFT. That is, the presence of IFT in the denominator of Ncr does not suffice to express the dependency of $(Y_g)_{Main}$ on IFT. Many different options were considered for the functional form of $(Y_g)_{Main}$ to the pertaining parameters and finally all the calculated $(Y_g)_{Main}$ values were

transferred onto a single curve by defining a new parameter for the x-axis of $(Y_g)_{Main}$, as follows:

$$(Y_g)_{Main} = F(x)$$
$$x = Ncr(IFTr)^{n_1} \tag{20}$$

where,
n_1: power exponent, to be determined by regression.
IFTr: ratio of base IFT to current IFT.

During this exercise we also considered the possibility of correlating $(Y_g)_{Main}$ to velocity in the form of Reynolds number (Re), which is the ratio of inertial to viscous forces. The optimised power exponents for Re in x was found to be zero. This is a very encouraging finding as it confirms that the use of β, when modifying base and miscible k_r curves, is sufficient for expressing the effect of inertia for almost all experimentally measured data points hence, no need for $β_g$.

In Equation 20 (n_1) exponent was found to be primarily dependent on IFT and S_{wi}. The functional form expressing this dependency was determined as,

$$n_1 = \frac{C_1 A_1 + C_2 [\log(IFTr)]^{C_3}}{A_1 + C_2 [\log(IFTr)]^{C_3}} \tag{21}$$

$$A_1 = C_4 e^{C_5 S_{wi}}$$

where,
$$C_1 = 0.838$$
$$C_2 = 0.316$$
$$C_3 = 12$$
$$C_4 = 646$$
$$C_5 = -C_3 = -12$$

Throughout this exercise the functional form of each part was determined by the stepwise evaluation of the effects of the dominant parameters and then it was subjected to a comprehensive multiple-regression exercise to finalise the constants.

As it was mentioned earlier, this approach was based on transferring all the calculated $(Y_g)_{Main}$ values on to a single curve, which then could be expressed by one simple mathematical formulation as follows:

$$(Y_g)_{Main} = \frac{1 + C_6 x}{1 + C_6 x + A_2 x^2} \tag{22}$$

where,
$$C_6 = -0.269$$
$$A_2 = C_7 e^{\left[\frac{c_8}{k\sqrt{\beta}}\right]}$$
$$C_7 = 0.111$$
$$C_8 = -50$$
$$x = \log\left[Ncr(IFTr)^{n_1}\right] \text{ with } (n_1) \text{ calculated from Equation 21.}$$

In this part to ensure a more consistent trend for the functional form of C_7, experimental data on the Texas Cream carbonate core were also used. That is, for the Texas Cream core data the same constants as those determined from the analysis of Clashach and Berea cores, i.e. C_1 to C_4 in Equation 21 and C_5 & C_6 in Equation 22, were used and the only variable to be determined was C_7.

Figure 3 is the plot of $(Y_g)_{Main}$ calculated by Equation 19 using measured k_{rg} data for Clashach core tests together with the best-fitted curve calculated using Equation 21.

As it was mentioned earlier there is also an extra term in the correlation to account for the effect of micro-pores in the core. Figure 4 demonstrates that the difference between the calculated $(Y_g)_{Main}$, Equation 22, and the corresponding values estimated by using measured k_{rg} values at the same GTR, Equation 21, can be expressed by a simple straight line. This difference, which is due to micro-pore effect, is labelled hereafter as $(Y_g)_{MicPoeff}$. Hence, the weight function, which modifies the predicted value by $(Y_g)_{Main}$ for the micro-pore effect and can be used for all the data pints is obtained by,

$$\left(Y_g\right)_{All} = \left(Y_g\right)_{Main} - \left(Y_g\right)_{MicPoeff} . \tag{23}$$

The limit and extent of $(Y_g)_{MicPoeff}$ is a function of GTR, IFT and the percentage of micro-pores in the core. The fraction of pores filled with the wetting phase at capillary pressure corresponding to the radius value of one micron $(S_{w1\,m})$ obtained from mercury porosimetry P_c curve has been considered to reflect the amount of small pores in the core. This value for Clashach core is 0.032. The corresponding value for the Berea core with a larger range of GTR affected by this effect increases to 0.232. However, for cores with very high percentage of small pores, e.g. Texas Cream core with $S_{w1\,m}=0.430$, even at the base IFT of 0.852 mNm^{-1} the flow of gas is not affected by the flow of condensate and $(k_{rgb})_{meas}$ values are close to unity Figure 5.

The proposed functional form of $(Y_g)_{MicPoeff}$, is expressed by,

$$\left(Y_g\right)_{MicPoeff} = (C_9 + C_{10}x)A_3A_4 . \tag{24}$$

where,

$C_9 = -0.3$

$C_{10} = 1.23$

$x = \log\left[Ncr(IFTr)^{n_1}\right]$ with (n_1) calculated from Equation 21.

In Equation 24, A_3 limits this effect to the corresponding GTR and IFT values for the cores with low and moderate percentage of micro-pores (e.g. Clashach and Berea cores) by the following equation:

$$A_3 = \left[\frac{C_{11}{}^2 + GTR^{A_3}}{C_{11} + GTR^{A_3}}\right] \tag{25}$$

$$A_5 = C_{12}\left[1 - S_{w1\mu m}\left(\frac{C_{13}}{S_{w1\mu m}}\right)\right]^{C_{14}} + \frac{C_{15}S_{w1\mu m}\left(\frac{C_{13}}{S_{w1\mu m}}\right)e^{\left(\frac{c_{16}}{IFTr}\right)}}{\left(1 - S_{wi}\right)^{C_{14}}}$$

where,

$C_{11} = 1E - 5$

$C_{12} = 4E + 3$

$C_{13} = 0.01$

$C_{14} = 4$

$C_{15} = 150$

$C_{16} = 10.$

In Equation 24, A_4 restricts the application of this term to the core types with high percentage of micro-pores (e.g. Texas Cream core) and is expressed by:

$$A_4 = \left[\frac{1 + S_{w1\mu m}{}^{C_{18}}}{C_{17} + S_{w1\mu m}{}^{C_{18}}}\right] \tag{26}$$

where,

$C_{17} = \dfrac{1}{C_{11}} = 1E + 5$

$C_{18} = -9.5$

Error Analysis

The Average absolute percentage deviation (AAD%) values expressing the error estimates in this section is calculated using the following equation:

$$AAD\% = \frac{\sum_{j=1}^{n}\left(\frac{abs\left[\left(k_{rg}\right)_{meas} - \left(k_{rg}\right)_{pred}\right]}{\left(k_{rg}\right)_{meas}}\right)_j}{n}*100 \tag{27}$$

where,

n: number of data points.

Subscripts (meas) and (pred) refer to permeability values measured in the core experiments and predicted by the correlation.

Using the $(Y_g)_{Main}$ expression, Equation 22, resulted in an AAD of 14% for all the data, including those deviating from the main trend. The deviation was reduced to 11% after implementing the microporosity correction term, Equation 24, in our calculation, Equation 23.

This might lead to the conclusion that the improvement in the accuracy of the correlation by adding the extra term is not significant, which would only be valid if the performance of reservoir is not greatly affected by this region of high GTR values. However the maximum observed deviations at high GTR due to microporosity was at 53%, without the additional term. The additional term reduced the deviation hugely at such conditions with a maximum AAD of 8%. Therefore, the use of $(Y_g)_{All}$ is recommended in preference to $(Y_g)_{Main}$,

particularly for rocks which contain a significant fraction of microporosity.

The accuracy of the correlation has also been examined for the available measured data on Texas Cream carbonate and two sandstone reservoir core samples. Tables 5 and 6 summarise the basic test data for the measurements conducted on these cores. These two tables also contain the results of error analysis. Note that AAD% of predicted k_{rg} values for these cores, with their measured k_r values not having been used in the development of the correlation, are the same as those of the previous cores. The low AAD% values for these cores with characteristics that are different to those used in developing the correlation are very encouraging for extending the use of this correlation to other cores.

Figures 6 and 7 are plots of measured and predicted k_{rg} at IFT values of 0.852 and 0.149 mNm^{-1} for RC2 core sample at two different velocities at which the inertia as well as coupling is affecting the measurements. Note a close agreement between the measured and corresponding predicted k_{rg} values over the entire range of fractional flow.

The performance of this correlation has also been compared with that of a saturation based correlation developed previously by this laboratory[19] and currently available in major commercially available reservoir simulators. The AAD% values reported in column 7 of Table 7 are the error values estimated using the saturation-based correlation with the corresponding core specific constants determined for these cores in this Laboratory. The corresponding AAD% values in columns 8 are those obtained using the present fractional flow based correlation using $(Y_g)_{All}$ formulation, Equation 23. These data indicate that the AAD% values obtained by saturation-based correlation, column 7, are mostly higher than those obtained by the fractional flow based correlation, column 8. Furthermore, it should be remembered that in the former correlation there are core specific coefficients, which should be determined through some expensive measurements, whilst in the latter one the coefficients are independent of the core type, which makes this new approach highly favorable.

Conclusions

A new relative permeability correlation, which combines positive coupling and negative inertial effects and accounts for micro-pores has been developed. The new k_{rg} correlation interpolates between k_{rgb} and k_{rgm} curves both as a function of fractional flow. The definition of fractional flow ties k_{rL} to k_{rg} thus eliminates the need for a separate correlation for k_{rL}. The k_{rgm} curve is modified to include the inertial effect using single-phase inertial factor, Equation 12. k_{rgb} is a measured curve at the lowest velocity level and the highest IFT value corrected for the effect of inertia, Equation 15. A generalized interpolating parameter $(Y_g)_{All}$, Equation 23, has been developed and correlated to commonly available petrophysical rock properties. Although specific core data have been used in developing the correlation, the results indicate the generality of the correlation.

In summary the new combined approach resulted in a general, more accurate, practically more efficient and physically more-sound formulation.

References
1. Danesh, A., Krinis, A., Henderson, G.D., Peden, J.M.: "Visual Investigation of the Retrograde Phenomena and Gas Condensate Flow in Porous Media," 5th EOR Europian Symposium, Budapest, 25-27 April 1989.
2. Bardon, C. and Longeron, D.G.: Influence of Very Low Interfacial Tension On Relative Permeability," *SPEJ*, Oct. 1980, 391-401.
3. Asar, H. and Handy, L. L.: "Influence of interfacial tension on gas/oil relative permeability in a gas-condensate system," *SPE* **11740**, *SPERE*, Feb. 1988, 264-275.
4. Haniff, M.S. and Ali, J.K.: "Relative permeability and low tension fluid flow in gas condensate systems," *SPE* **20917**, *European petroleum conference*, 21-24 Oct. 1990, proceedings' page 351-358.
5. Munkerud, P. K.: "The effect of interfacial tension and spreading on relative permeability in gas condensate systems," *In Proc. 8th European IOR Symposium*, Vienna, 15-17 May 1995, proceedings' page 241-260.
6. Danesh, A., khazam, M., Henderson, G.D., Tehrani, D.H., Peden, J.M.: "Gas Condensate recovery studies," *DTI Improved Oil Recovery and Research Dissemination Seminar*, London, June 1994.
7. Henderson, G.D., Danesh, A., Tehrani, D.H., Peden, J.M.: "The effect of velocity and interfacial tension on the relative permeability of gas condensate fluids in the wellbore region," presented at the *8th IOR European Symposium,* Vienna, May 1995, proceedings' page 201-208.
8. Henderson, G.D., Danesh, A., Tehrani, D.H., Peden, J.M.: "Measurement and correlation of gas condensate relative permeability by the steady-state method," *SPEJ*, June 1996, 191-201.
9. Ali J. K., McGauley, P. J., and Wilson, C. J.: "The effects of high velocity flow and PVT changes near the wellbore on condensate well performance," *SPE* **38923**, *SPE Annual Technical Conference and Exhibition*, 5-8 Oct. 1997, proceedings' page 823-838.
10. Blom, S.M.P., Hagoort, J. and Soetekouw, D.P.N.: "Relative permeability near welbore conditions," *SPE* **38935**, *SPE Annual Technical Conference and Exhibition*, 5-8 Oct. 1997, proceedings' page 957-967.
11. Jamiolahmady, M., Danesh, A., Tehrani, D. H. and Duncan, D. B.: "A mechanistic model of gas-condensate flow in pores," *Transport in Porous Media*, Oct. 2000, **41** (1), 17-46.

12. Jamiolahmady, M., Danesh, A., Tehrani, D. H. and Duncan, D. B.: "A mechanistic model of gas-condensate flow in pores," *Transport in Porous Media*, Aug. 2003, **52** (2), 159-183.

13. Blom, S.M.P. and Hagoort, J., "The combined effect of near-critical relative permeability and non-Darcy flow on well impairment by condensate drop out," *SPE* **51367**, *SPERE*, Oct. 1998, 421-429.

14. Henderson, G.D., Danesh, A., Badr Al-kharusi, Tehrani, D.H.: "Generating reliable gas condensate relative permeability data used to develop a correlation with capillary number," Journal of *Petroleum Science and Engineering*, 25, 2000, 79-91.

15. Eclipse Reference Manuals, Version 2002A, **2002**, Technical Description, Chapter, 6-10, Schlumberger.

16. VIP Technical Reference Manuals, version 2003.R4, **2002**, Executive Technical Reference, Chapter 35, 495-507, Landmark Graphic Corporation.

17. Blom, S.M.P. and Hagoort, J.: "How to include the capillary number in gas condensate relative permeability functions?," *SPE* **49268,** *SPE Annual Technical Conference and Exhibition,* Louisiana, 27-30 Sept. 1998, proceedings' page 661-671.

18. Henderson, G.D., Danesh, A., Tehrani, D.H.: "Effect of positive rate sensitivity and inertia on gas condensate relative permeability at high velocity," *Petroleum Geoscience*, 2001, Vol. 7, 45-50.

19. Henderson, G.D., Danesh, A., Tehrani, D.H., Badr Al-kharusi: "The relative significance of positive coupling and inertial effects on gas condensate relative permeabilities at high velocity," *SPE* **62933,** *SPE Annual Technical Conference and Exhibition,* Dallas, 3-6 Oct. 2000, proceedings' page 193-202.

20. Whitson, C. H., Fevang, O., Saevareid, A.: "Gas condensate relative permeability for well calculations," *SPE* **56476,** *SPE Annual Technical Conference and Exhibition* Texas, 3-6 Oct. 1999.

21. App, J.F. and Mohanty, M.: "Gas and condensate relative permeability at near critical conditions: capillary and Reynolds number dependence," Journal of Petroleum Science and Engineering, 2002, **36**, 111-126.

22. Dacun, L. and Thomas, W.E.: "Literature review on correlations of the non-Darcy coefficient," *SPE* **70015,** presented at the 2001 *Permian Basin oil and gas recovery conference,* Texas, 15-17 May.

23. Al-Kharusi, S.B.: Relative permeability of gas-condensate near wellbore, and gas-condensate-water in bulk of reservoir, *PhD thesis,* Heriot-Watt University, 2000.

24. Danesh, A., Tehrani, D.H., Henderson, G.D., Jamiolahmady, M., Ataei R., Ireland S.: "Gas Condensate recovery studies," *DTI Improved Oil Recovery and Research Dissemination Seminar*, London, June 2002.

25. 8. Coles, M.E., and Hartman, K.J.: "Non-Darcy measurements in dry core and the effect of immobile liquid," **SPE 39977,** *SPE Gas Technology Symposium*, 15-18 Mar. 1998, Calgery, proceeding's page 193-202.

Nomenclature

C_j =constant, j=1 to 18
k =absolute permeability

$k(S_{wi})$ =permeability at S_{wi}
k_e =effective permeability
k_r =relative permeability
L =length
n_l =power exponent
n =number of points
P_c =capillary pressure
Q =flow rate
S_{wi} =immobile water saturation, fraction
$S_{w1\ m}$ =wetting phase (air) saturation corresponding to one micron radius from mercury porosimetry P_c curve
V =velocity
Y =weight function for interpolation of k_r
$(Y_g)_{Main}$ =gas weight function for majority of data points following main trend
$(Y_g)_{MicPoEff}$=gas weight function for data points not following main trend due to effect of micro-pores
$(Y_g)_{All}$ =gas weight function for all data points

Greek Letters.
β =single phase inertial factor
$\beta(S_{wi})$ =single phase inertial factor at S_{wi}
β_g =two phase inertial factor for gas phase
ϕ =porosity of porous medium, fraction
μ =viscosity
ρ =density
σ =interfacial tension between gas and liquid

Subscript.
ave   =denotes average value of the quantity
b   =denotes the value of the quantity for the base case at highest measured interfacial tension, IFT=0.852 mNm^{-1} and lowest velocity
g   =refers to gas phase
iner   =denotes value of the quantity affected by inertia
j   =an index
L   =refers to liquid (i.e. condensate)
m   =denotes the value of the quantity for the miscible case
T   =denotes the value of the quantity to that of summation of gas and liquid
meas =refers to measured value of the quantity
pred   =refers to calculated value of the quantity by the correlation
sm   =denotes the value of the quantity for the total miscible gas and liquid phases considered as a single flowing phase

Abbreviations.
CGR   =condensate to gas flow rate ratio
GTR   =gas to total flow rate ratio
IFT   =interfacial tension
IFTr   =ratio of base IFT of 0.852 mNm^{-1} to current IFT
Nc   =capillary number, ratio of viscous to capillary forces
Ncr   =ratio of current Nc to base Nc
Re   =Reynolds number, ratio of inertial to viscous forces
Vel   =Velocity

Operators.

∇ =gradient operator

Δ =difference

| | =absolute value

Table 1:   Basic test data for the experiments conducted on Clashach cores at different conditions.

Index	S_{wi} %	k /mD	$k(S_{wi})$ /mD	IFT /mNm^{-1}	β /m^{-1}	$\beta (S_{wi})$ /m^{-1}
1	0	553	---	0.852	1.035E8	---
2	0	553	---	0.149	1.035E8	---
3	0	553	---	0.036	1.035E8	---
4	0	600	---	0.149	5.990E7	---
5	0	600	---	0.036	5.990E7	---
6	33	553	245	0.852	1.035E8	4.580E8
7	21	553	446	0.852	1.035E8	1.395E8*
8	21	553	446	0.149	1.035E8	1.395E8*
9	15	440	400	0.852	1.035E8	1.151E8*
10	15	440	400	0.149	1.035E8	1.151E8*
11	15	440	400	0.008	1.035E8	1.151E8*

S_{wi} is the immobile water saturation and $k(S_{wi})$ and $\beta(S_{wi})$ are the phase permeability and inertia factor, respectively, of the core sample at S_{wi}.
* Calculated $\beta(S_{wi})$ values, Equation 17.

Table 2:   Basic test data for the experiments conducted on Berea cores at different conditions.

Index	S_{wi} %	k /mD	$k(S_{wi})$ /mD	IFT /mNm^{-1}
12	0	110	---	0.852
13	0	110	---	0.149
14	0	110	---	0.036
15	0	116	---	0.008
16	26	110	92	0.852
17	26	110	92	0.448
18	26	110	92	0.149
19	26	110	92	0.036
20	26	110	92	0.008

For Berea core sample β/m^{-1}=1.870E8 was measured experimentally and $\beta(S_{wi}=26\%)$/m^{-1}=2.286E8 was calculated using Equation 17. See footnotes of Table 1.

Table 3:   Basic test data for the experiments conducted on Clashach cores at different conditions.

Index*	Base Total Pore Vel. /md^{-1}	No. of Vel.	Highest GTR Following Main Trend	Deviating GTR & (Its Category)
1	7.28	10	0.971	0.995,0.990 (2)
2	7.28	10	0.981	0.995 (1)
3	7.28	7	0.971	0.995 (1)
4	7.05	10	0.981	
5	7.05	10	0.971	
6	10.87	10	0.991	
7	9.22	10	0.991	0.995 (1)
8	9.22	9	0.981	0.995 (1)
9	9.36	4	0.981	0.995 (1)
10	9.36	4	0.991	
11	9.36	4	0.971	0.995 (1)

* Indexes correspond to those shown in Table 1.

Table 4:   Basic test data for the experiments conducted on Berea cores at different conditions.

Index*	Base Total pore Vel. /md^{-1}	No. of Vel.	Highest GTR Following Main Trend	Deviating GTR & (Its Category)
12	7.09	8	0.910	0.995,0.971 (2)
13	7.09	9	0.971	0.995, 0.990, 0.981 (1)
14	7.09	6	0.910	0.990, 0.971, 0.952 (1)
15	6.41	4	0.910	0.990, 0.971 (1)
16	9.21	4	0.995	
17	9.21	4	0.995	
18	10.81	4	0.981	
19	9.21	4	0.971	
20	9.21	4	0.971	0.995, 0.981 (1)

* Indexes correspond to those shown in Table 2.

Table 5: Error analysis of k_{rg} formulations conducted on Texas Cream cores at different conditions.

Index	S_{wi} %	k /mD	$k(S_{wi})$ /mD	IFT mNm^{-1}	Base Total Pore Vel. /md^{-1}	No. of Vel.	AAD% k_{rg}
21	0	9.1	---	0.852	6.0	7	6
22	0	11.1	---	0.149	5.3	4	13
							9
23	22	11.1	8.4	0.149	7.2	4	14
24	22	11.1	8.4	0.036	7.2	4	11
							13
Ave. (with & without S_{wi})							11

For Texas Cream core sample β/m^{-1}=3.927E9 was measured experimentally and $\beta(S_{wi}=22\%)/m^{-1}$=5.933E9 was calculated using Equation 17. See footnotes of Table 1.

Table 6: Error analysis of k_{rg} formulations conducted on TotalFinaElf core at different conditions.

Index	Core Type	S_{wi} %	IFT mNm^{-1}	Base Total Pore Vel. /md^{-1}	No. of Vel.	AAD% k_{rg}
25		0	0.852	7.0	4	11
26	RC1b	0	0.149	7.0	1	23
27		0	0.036	0.7	2	9
Ave.						13
28		0	0.852	3.4	7	12
29		0	0.149	6.7	6	16
30	RC2	0	0.036	6.7	5	11
Ave.						13
31		33	0.852	10.0	6	17
Ave. ALL (with & without S_{wi})						14

K=0.18 mD for Rc1b, k=11 mD for RC2 & $k(S_{wi})$=7.6 mD for RC2 core test indexed 31. β/m^{-1}=1.056E12 for Rc1b core sample and β/m^{-1}=1.623E10 for RC2 core sample were measured experimentally. $\beta(S_{wi}=33\%)/m^{-1}$=2.527E10 for wet Rc2 core sample was calculated using Equation 17. See footnotes of Table 1.

Table 7: Average absolute percentage deviation (AAD%) of k_{rg} for Clashach and Berea cores.

Core Type & (S_{wi})	k /mD	$k(S_{wi})$ /mD	β /m^{-1}	$\beta(S_{wi})$ /m^{-1}	AAD% k_{rg} **	AAD% k_{rg} Eq. 23
C (0%)	553	---	1.035E8	---	16	10
C (0%)	600	---	5.990E7	---	21	14
C (33%)	553	245	1.035E8	4.580E8	12	18
C (21%)	553	446	1.035E8	1.395E8*	17	18
B (0%)	110	---	1.870E8	---	14	9

Index C & B refer to Clashach and Berea cores, respectively. ** Saturation based correlation in Eclipse. See footnotes of Table 1.
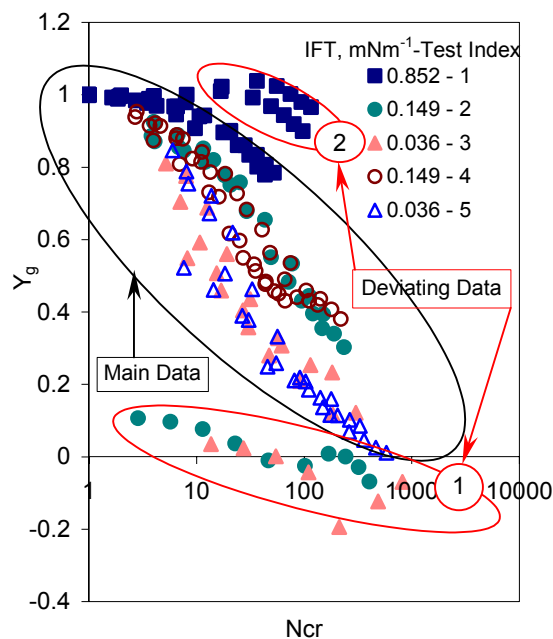

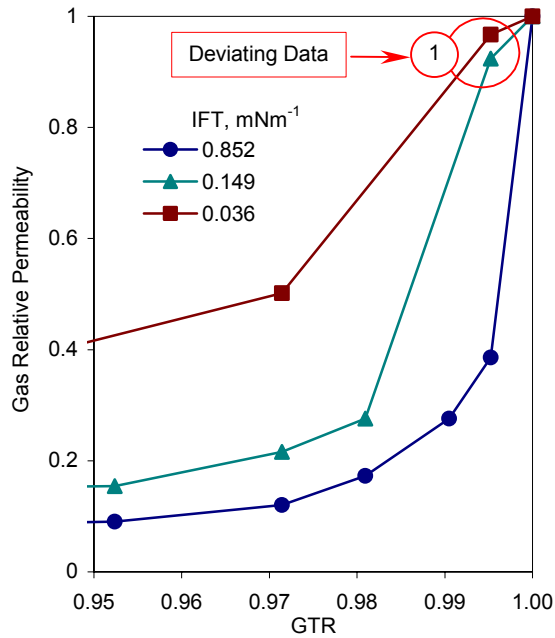Figure 1: Y_g vs. Ncr for different Clashach core tests, S_{wi}=0%.

Figure 2: Gas relative permeability vs. gas to total fractional flow rate (GTR) for Clashach core at three different IFT values, S_{wi}=0% & Velocity=7.3 md^{-1}.
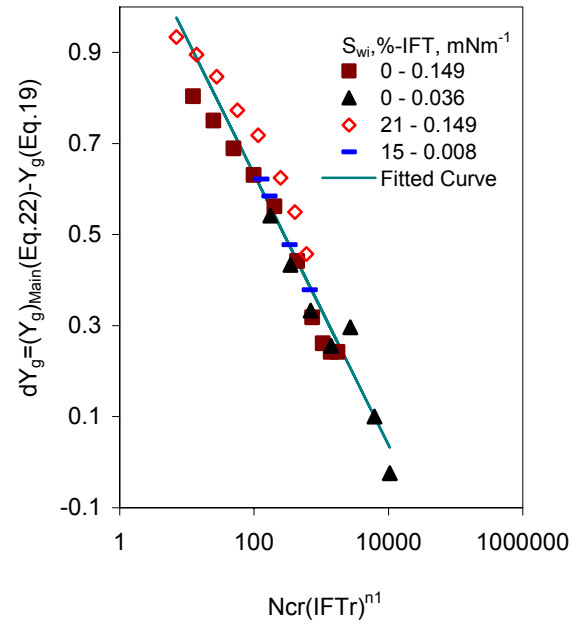

Figure 4: dY_g vs. $Ncr(IFTr)^{n1}$ product for data of Clashach core tests at GTR=0.995, which are affected by micro-pores.
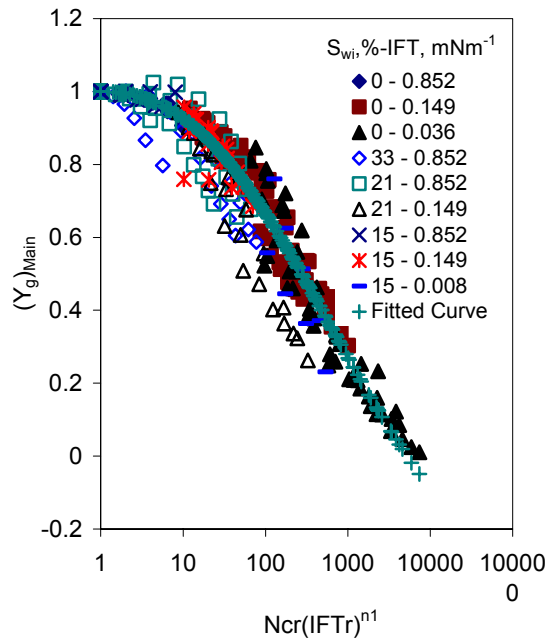

Figure 3: $(Y_g)_{Main}$ vs. $Ncr(IFTr)^{n1}$ product for Clashach core tests, with n_1 calculated using Equation 21, together with best fitted-curve, Equation 22.
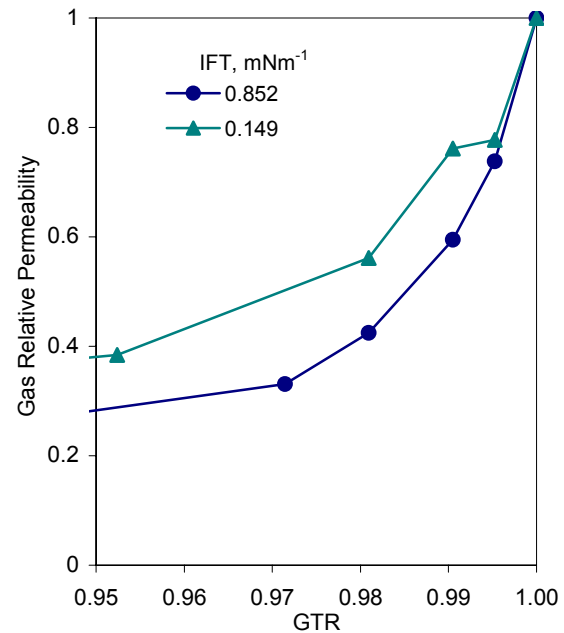

Figure 5: Gas relative permeability vs. gas to total fractional flow rate (GTR) for Texas Cream core at two different IFT values, S_{wi}=0% & Velocity=5.6 md^{-1}.
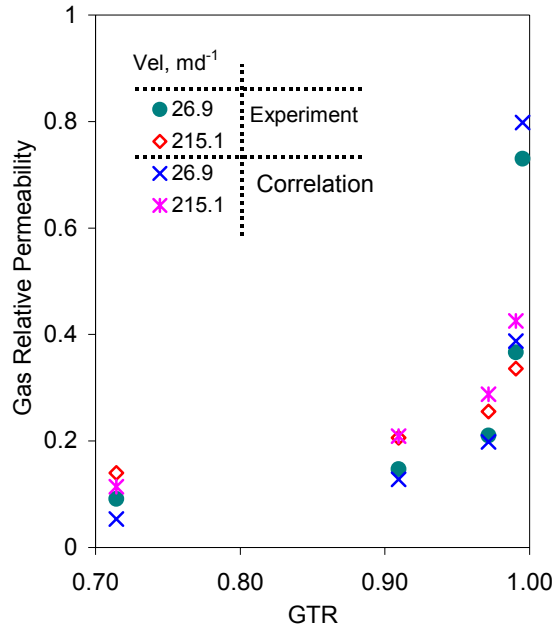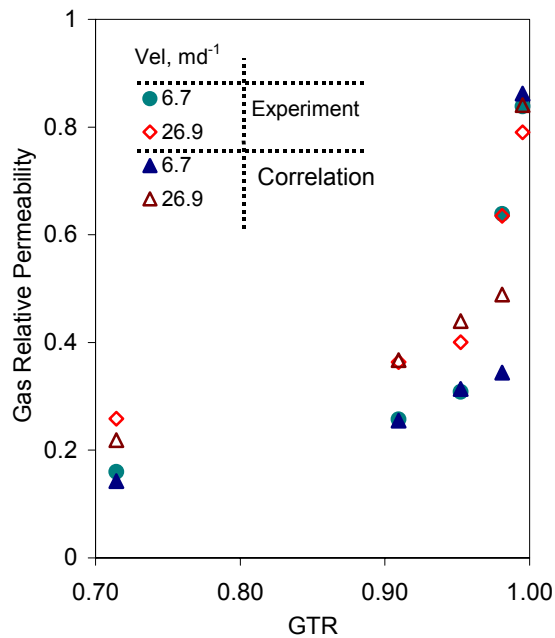
Figure 6: Gas relative permeability measured in the core experiments and predicted by the correlation vs. gas to total fractional flow rate (GTR) for RC2 core at two different velocity values, S_{wi}=0% & **IFT=0.852 mNm^{-1}**.

Figure 7: Gas relative permeability measured in the core experiments and predicted by the correlation vs. gas to total fractional flow rate (GTR) for RC2 core at two different velocity values, S_{wi}=0% & **IFT=0.149 mNm^{-1}**.